TISSUE ENGINEERING: Part C
Volume 22, Number 5, 2016

DOI: 10.1089/ten.tec.2015.0556

termis
Tissue Engineering
& Regenerative Medicine
International Society

METHODS ARTICLE

Customized Interface Biofunctionalization of Decellularized Extracellular Matrix: Toward Enhanced Endothelialization

Hug Aubin, MD,[1,2] Carlos Mas-Moruno, PhD,[3,4] Makoto Iijima, MD,[2] Nicolas Schütterle,[2] Meike Steinbrink,[2] Alexander Assmann, MD,[1,2] Francesc Javier Gil, PhD,[3,4] Artur Lichtenberg, MD,[1,2] Marta Pegueroles, PhD,[3,4] and Payam Akhyari, MD[1,2]

Interface biofunctionalization strategies try to enhance and control the interaction between implants and host organism. Decellularized extracellular matrix (dECM) is widely used as a platform for bioengineering of medical implants, having shown its suitability in a variety of preclinical as well as clinical models. In this study, specifically designed, custom-made synthetic peptides were used to functionalize dECM with different cell adhesive sequences (RGD, REDV, and YIGSR). Effects on *in vitro* endothelial cell adhesion and *in vivo* endothelialization were evaluated in standardized models using decellularized ovine pulmonary heart valve cusps (dPVCs) and decellularized aortic grafts (dAoGs), respectively. Contact angle measurements and fluorescent labeling of custom-made peptides showed successful functionalization of dPVCs and dAoGs. The functionalization of dPVCs with a combination of bioactive sequences significantly increased *in vitro* human umbilical vein endothelial cell adhesion compared to nonfunctionalized controls. In a functional rodent aortic transplantation model, fluorescent-labeled peptides on dAoGs were persistent up to 10 days *in vivo* under exposure to systemic circulation. Although there was a trend toward enhanced *in vivo* endothelialization of functionalized grafts compared to nonfunctionalized controls, there was no statistical significance and a large biological variability in both groups. Despite failing to show a clear biological effect in the used *in vivo* model system, our initial findings do suggest that endothelialization onto dECM may be modulated by customized interface biofunctionalization using the presented method. Since bioactive sequences within the dECM–synthetic peptide platform are easily interchangeable and combinable, further control of host cell proliferation, function, and differentiation seems to be feasible, possibly paving the way to a new generation of multifunctional dECM scaffolds for regenerative medicine.

Introduction

Native extracellular matrix (ECM) can be decellularized by standard detergent-based protocols under high preservation of its ultrastructural composition and microarchitecture[1] while eliminating cell-based antigens, such as α-Gal-epitopes or human leukocyte antigens,[2] which may trigger undesired immune response upon implantation to a host organism.[3] Therefore, decellularized ECM (dECM) is widely used as a platform for bioengineering of medical implants, having shown its suitability in a variety of preclinical as well as clinical models.[4–8]

In the cardiovascular field, dECM-based approaches are particularly pursued in heart valve and vascular graft engineering.[4] Here, experimental models have already successfully been translated into the preclinical and clinical settings, with, for example, a first clinical series of decellularized allogenic valves implanted in the pulmonary as well as aortic positions showing promising mid- and long-term results.[5,9] However, early graft failure due to severe calcification, thrombogenesis, and immune response mechanisms has also been reported in the past.[10] Those adverse reactions may have been triggered not only by remnants of immunogenic donor material due to incomplete decellularization[11] but

[1]Department of Cardiovascular Surgery, Heinrich-Heine University Düsseldorf, Düsseldorf, Germany.
[2]Research Group for Experimental Surgery, Department of Cardiovascular Surgery, Medical Faculty, Heinrich-Heine University Düsseldorf, Düsseldorf, Germany.
[3]Biomaterials, Biomechanics and Tissue Engineering Group, Department of Materials Science and Metallurgical Engineering, Technical University of Catalonia (UPC), Barcelona, Spain.
[4]Center for Research in NanoEngineering (CRNE), Technical University of Catalonia (UPC), Barcelona, Spain.

also by nonautologous ECM components lying on the free graft surface.[12] Therefore, early functional autologous endothelialization is crucial for all ECM surfaces in direct contact with the bloodstream. Particularly in the case of decellularized vascular grafts (dVGs), this is of utmost importance as insufficient or nonfunctional luminal endothelialization and adverse neovessel remodeling may lead to early and late graft failure,[13] preventing dVGs from reaching clinical suitability despite having already been successfully tested in a multitude of experimental models.[13,14]

Interface biofunctionalization strategies aim to modulate and control the interaction between implants and host organisms to enhance biocompatibility of implant materials and potentially even regulate implant function. Surface functionalization with ECM- or growth factor-derived molecules is a commonly used and feasible approach to improve host cell–scaffold interactions at the interface level and enhance the biointegration of implant materials.[15–18] In the past, surface coating of engineered vascular grafts with bioactive proteins, such as fibronectin, fibrin, or vascular endothelial growth factor, has been shown to accelerate the autologous recellularization and improve graft function.[19–21] However, protein-based strategies may not lead to functional endothelium or prevent neointimal hyperplasia as they have been proven insufficient to elicit specific biological cues required in the process of neoendothelium formation.[21] In particular, a biological blood–graft interface with high endothelial cell (EC) specificity, while suppressing activation of platelet attachment, immune cell recruitment, and smooth muscle cell overproliferation, is crucial in the process of *in vivo* endothelialization.[22]

In this regard, cell-specific surface functionalization can be achieved using short synthetic peptides with defined bioactive sequences.[15,23] Interestingly, custom-made peptides, which are derived from ECM proteins but encompass only defined cell adhesive motifs, offer a series of advantages compared to the use of native proteins: they are chemically defined structures, show higher stability, and are devoid of immunogenicity.[24] Moreover, distinct bioactive peptides can be combined to exert synergistic or complementary effects on the surface of an implant.[25] Therefore, in this study, we specifically designed and synthesized custom-made synthetic peptides with the following cell adhesive sequences to functionalize dECM:

- Arg-Gly-Asp (RGD)—present in fibronectin and other proteins, critical component for mediating general cell adhesion[26,27]
- Arg-Glu-Asp-Val (REDV)—adhesion ligand located in the type III connecting segment domain of human plasma fibronectin, targeting integrin $\alpha_4\beta_1$, which is widely expressed on ECs[28,29]
- Tyr-Ile-Gly-Ser-Arg (YIGSR)—a nonintegrin binding peptide sequence present in laminin, which promotes EC adhesion.[28,30]

All selected amino acid sequences are derived from ubiquitous ECM proteins of native tissues, such as fibronectin and laminin. Additionally, REDV and YIGSR specifically mediate adhesion and migration of ECs while preventing platelet adhesion.[28,31]

In this proof-of-concept study, the feasibility of dECM biofunctionalization with custom-made synthetic peptides and biological effects of selected bioactive sequences on *in vitro* EC adhesion and *in vivo* endothelialization were evaluated in standardized models using decellularized ovine pulmonary heart valve cusps (dPVCs) and decellularized aortic grafts (dAoGs), respectively. We further hypothesized that a combination of bioactive motifs may create higher EC specificity than coating with single agents and, thus, may increase the biological potential of functionalized dECM platforms.

Materials and Methods

All animal experiments and surgical procedures were performed in compliance with the Guide for the Care and Use of Laboratory Animals as published by the US National Institutes of Health (NIH Publication 85-23, revised 1996) and approved by the local animal care committees (Registration No. A/391/2012).

Design and synthesis of custom-made synthetic peptides

Custom-made RGD, REDV, and YIGSR cell adhesive peptides were designed as shown in Figure 1. The synthetic peptides contained a spacing-anchoring moiety composed of three units of aminohexanoic acid and one residue of mercaptopropionic acid to ensure an appropriate orientation of the motifs and binding within the dECM substrates.[32,33] The peptides were manually synthesized in solid phase (2-chlorotrityl chloride resin, 200 mg, 1.0 mmol/g) following the Fmoc/tBu strategy according to a previously reported protocol.[25] In brief, Fmoc-L-amino acids were sequentially coupled at a four equivalent excess using either OxymaPure/N,N′-diisopropylcarbodiimide (DIC) or HATU/N,N-diisopropylethylamine (DIEA) as coupling systems.[34] The efficiency of each coupling step was monitored using the Kaiser test and/or by high-performance liquid chromatography (HPLC) analysis. Fluorescent-labeled peptides were obtained by acylation of the N-terminus with 5(6)-carboxyfluorescein.[35] In this case, mercaptopropionic acid was substituted by a cysteine residue incorporated at the C-terminus of the sequence. All peptides were cleaved from the resin with trifluoroacetic acid (TFA)–water–triisopropylsilane (TIS) (85:10:5, v/v/v) for 1–2 h in the presence of dithiothreitol (DTT). The peptides were purified by semipreparative HPLC and characterized by analytical HPLC using a reversed-phase XBridge BEH130 C-18 column (4.6 × 100 mm, 3.5 μm) (Waters, Milford, MA) and a photodiode array detector (Waters 2998), and mass spectra were recorded on a MALDI-TOF Voyager DE RP spectrometer (Applied Biosystems, Foster City, CA) (Table 1). All chemicals required for the synthesis, including resins, Fmoc-L-amino acids, and coupling reagents, were obtained from Iris Biotech GmbH (Marktredwitz, Germany) and Sigma-Aldrich (St. Louis, MO).

ECM substrates and model systems

Different sources of ECM were used in this proof-of-concept study, relying on well-characterized dECM substrates and previously established model systems. Functionalization capacity of dECM was first evaluated on ovine pulmonary vascular cusps (PVCs)[6] and ovine pericardium (OP),[2] representing clinically relevant dECM substrates for heart valve engineering. Fresh bovine pericardial tissue (control bovine

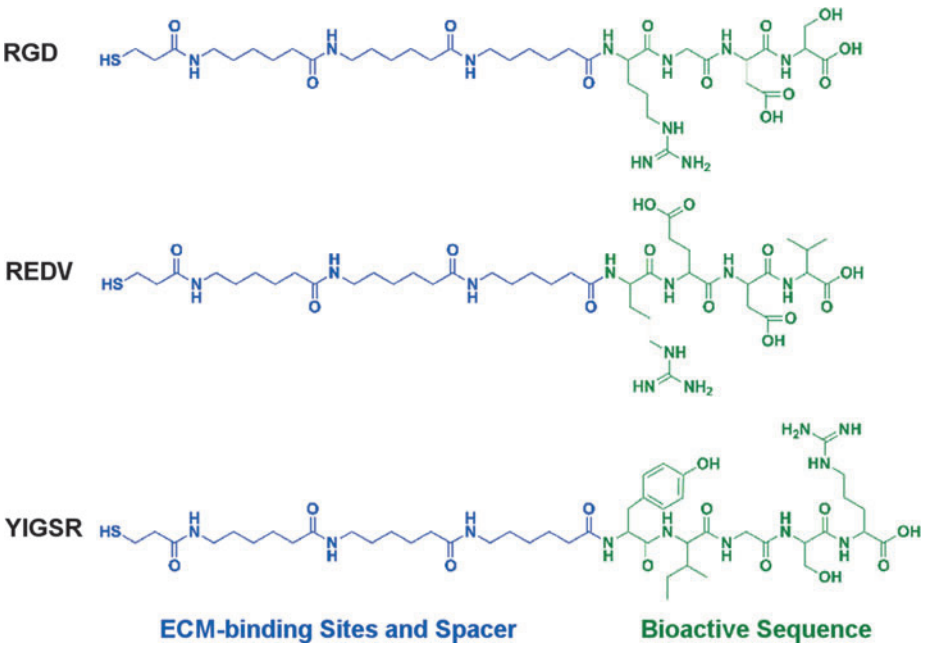

FIG. 1. Custom-made synthetic peptides. Chemical structure of custom-made synthetic peptides containing a spacing-anchoring moiety composed of three units of aminohexanoic acid and one residue of mercaptopropionic acid (highlighted in *blue*) as well as the respective bioactive amino acid sequence (highlighted in *green*). RGD, Arg-Gly-Asp; REDV, Arg-Glu-Asp-Val; YIGSR, Tyr-Ile-Gly-Ser-Arg. Color images available online at www.liebertpub.com/tec

pericardium [cBP]) stored in a propylalcoholic solution containing EDTA was used as a control, representing an analog to commercially available and chemically preserved ECM.[36] After initially confirming the feasibility of the dECM functionalization strategy, biological effects were assessed *in vitro* in a standardized model system for cell adhesion onto dPVCs, as previously described,[37] and *in vivo* in a functional rodent aortic graft (AoG) transplantation model, a standardized vascular graft model system allowing the *in vivo* evaluation under systemic pressure, as previously described.[7]

Decellularization of ECM. All ECM materials (except for the chemically preserved cBP) were decellularized on a detergent basis, as previously described.[2,7,36] Briefly, decellularization was achieved through dynamic tissue incubation in four repetitive 12-h cycles with 0.5% sodium dodecyl sulfate (SDS) and 0.5% deoxycholate (DCA), followed by 24 h of incubation in distilled water containing 0.05% sodium azide and three repetitive 24-h rinsing cycles with phosphate-buffered saline (PBS) and 1% penicillin/streptomycin. Decellularization quality was controlled as previously described.[38] All chemicals required were obtained from Sigma-Aldrich and Merck (Darmstadt, Germany).

Ovine PVCs. Ovine hearts were obtained from juvenile sheep (20–25 kg) at a local slaughterhouse and kept on ice until further processing at our research facility. Pulmonary heart valves were carefully dissected and decellularized in toto. After the decellularization process, the individual pulmonary heart valve cusps were harvested and stored in 4°C PBS with 1% penicillin/streptomycin until further processing.

Rodent AoGs. Rodent AoGs were harvested from donor Wistar rats (male, 200–250 g), essentially following a recent publication, with minor modifications.[7] Briefly, following CO_2 euthanization and thoracotomy, the thoracic and upper abdominal aorta were explanted in toto and thoroughly rinsed with heparinized PBS. A U-shaped AoG was prepared by dissection of adjacent connective tissue and clipping of the supra-aortal arteries. Harvested grafts were stored in 4°C PBS with 1% penicillin/streptomycin until further processing.

TABLE 1. CHEMICAL SEQUENCE AND CHARACTERIZATION OF THE PEPTIDES

Code	*Sequence*	t_R *(min)*[a]	*Purity (%)*[b]	*Calc. m/z*	*Exp. m/z*[b] *[M+H]*$^+$
RGD	MPA-$(Ahx)_3$-Gly-Arg-Gly-Asp-Ser-OH	4.227	97	917.46	918.29
REDV	MPA-$(Ahx)_3$-Arg-Glu-Asp-Val-OH	4.879	96	944.50	945.84
YIGSR	MPA-$(Ahx)_3$-Tyr-Ile-Gly-Ser-Arg-OH	5.503	95	1021.56	1022.94
CF-RGD	CF-Arg-Gly-Asp-Ser-$(Ahx)_3$-Cys-OH	6.421	98	1233.50	1234.84
CF-REDV	CF-Arg-Glu-Asp-Val-$(Ahx)_3$-Cys-OH	6.124	>99	1317.56	1319.72
CF-YIGSR	CF-Tyr-Ile-Gly-Ser-Arg-$(Ahx)_3$-Cys-OH	6.636	>99	1394.62	1396.79

[a]tR and purity of the peptides were calculated by analytical high-performance liquid chromatography with a photodiode array detector. Linear gradients, expressed as percentage of MeCN for 8 min under a 1.0 mL/min flow, were used as follows: RGD (10–40), REDV (10–50), YIGSR (10–50), CF-RGD (5–50), CF-REDV (5–60), and CF-YIGSR (5–60).
[b]Mass spectra were recorded on a MALDI-TOF (see text for details).
Ahx, aminohexanoic acid; CF, 5(6)-carboxyfluorescein; MPA, mercaptopropionic acid; tR, retention time.

Surface functionalization of dECM

Surface functionalization of dECM was performed by means of immersion and physical adsorption, as previously described, for the functionalization of synthetic surfaces.[25,39] Briefly, lyophilized bioactive peptides were reconstituted in PBS (pH 6.5), and dECM components were incubated for 12 h at room temperature under orbital agitation at 100 rpm in varying peptide concentrations (100, 200, and 500 μM). dECM incubated in plain PBS under the same conditions served as nonfunctionalized control. After the incubation period, samples were gently washed with PBS and ultrapure distilled water.

Contact angle measurement. For indirect proof of peptide adhesion onto the dECM, wettability measurements were performed before and after RGD functionalization. The apparent static contact angles (CAs) were measured for the air bubble/liquid/solid system, where the air bubble was deposited onto the solid surface with the captive bubble technique[40] (Supplementary Fig. S1; Supplementary Data are available online at www.liebertpub.com/tec). Three microliters of bubbles were generated with a micrometric syringe and deposited on the substrate surface placed upside down into a cuvette filled with distilled Milli-Q water. The wettability studies were performed with a CA video-based system (Contact Angle System OCA15plus; DataPhysics, Filderstadt, Germany) and analyzed with the SCA20 software (DataPhysics).

Fluorescent-labeled peptides. For direct proof of peptide attachment to the dECM, peptide platforms were modified to contain a fluorescent carboxyfluorescein group, as described in the ''Design and Synthesis of Custom-Made Synthetic Peptides'' section. The fluorescent-labeled peptides were then used for dECM functionalization as described above. Before visualization, samples were subjected to extensive (×10) washings in ultrapure distilled water to remove weakly adsorbed peptides off the surfaces. Labeled peptides on dECM surface were visualized *in vitro* and *ex vivo* by imaging with a fluorescent microscope (DM2000; Leica, Wetzlar, Germany) and the Leica Application Suite V3.7 software. Fluorescence intensity was measured by image processing using built-in functions of NIH ImageJ software.

In vitro *cell adhesion studies*

For *in vitro* cell adhesion studies on functionalized dPVCs, primary human umbilical vein endothelial cells (HUVECs) were used. HUVECs were cultured in a standard cell culture incubator (Thermo Scientific, Waltham, MA) in 5% CO_2 atmosphere and at 37°C, maintained in endothelial basal medium (EBM-2; PromoCell, Heidelberg, Germany) with according supplements and 1% penicillin/streptomycin, and passaged when 60–70% confluence was reached, while media were exchanged every second day.

Functionalized dPVCs were surface seeded with HUVECs (3×10^5 cells/mL) in a tailor-made ECM evaluation culture device (culture volume 300 μL) to ensure standardization, as previously described.[37] After 1 and 4 h, seeded dPVCs were washed 2× with PBS to wash off nonattached cells, stained with 2 μM calcein-AM (Invitrogen, Carlsbad, CA) for 30 min at 37°C, and fixed in 2% formaldehyde for 60 min. Samples were visualized with an inverted fluorescent microscope (DM IL LED; Leica), dividing the seeding area of each cusp into four quadrants recorded at 5× magnification. To account for in-sample inhomogeneity and variance, due to nonflat surface and fluorescence dispersion, each fluorescent picture (representing one fourth of one cusp) was converted into a 16-bit gray scale image and divided into 36 standardized rectangular regions of interest (ROIs). For each ROI, an individual threshold was adjusted, in order to visually distinguish the area occupied by cells from nonseeded ECM surface. The area occupied by cells was then measured for each ROI (total amount of pixels) and averaged for each sample using built-in functions of NIH ImageJ software.

In vivo *endothelialization studies*

For *in vivo* endothelialization studies, Wistar rats (male, 200–250 g) (from an in-house breed of the local animal care facility), fed *ad libitum* with standard rat chow, were used as a rodent model. Heterotopic implantation of the functionalized dAoGs into the systemic circulation of recipient rats was conducted according to a recent publication, with minor modifications.[7] Briefly, recipient rats were anesthetized with 2.0–2.5% isoflurane, orally intubated, and machine ventilated. After insertion of a central venous jugular vein catheter and systemic heparanization (100 IU/kg), a median laparotomy was performed, and the infrarenal aorta was dissected from the inferior vena cava. The abdominal aorta was clamped, and the graft was anastomosed to the infrarenal aorta in an end-to-side manner using a 10-0 monofilament nonabsorbable polypropylene suture (Ethicon, Norderstedt, Germany). Then, the native aorta between the two anastomoses was ligated to improve the graft perfusion, and the abdomen was closed in layers. Graft performance was evaluated directly after implantation and at explantation measuring peak systolic velocity (PSV max) at the proximal and distal graft ends with a Philips HDX11 ultrasonography system equipped with a 15-MHz probe (Philips, Hamburg, Germany).

Histological graft analysis. For histological graft analysis, explanted grafts were fixed in a 4% buffered formaldehyde solution (Carl Roth, Karlsruhe, Germany) and processed via cryostat sectioning (CM1950; Leica) using standard protocols. Frozen sections of 5 μm were then stained with hematoxylin and eosin (HE) and Movat's pentachrome staining according to standard protocols and then visualized using a transmission light microscope (DM2000; Leica).

For quantitative analysis of percentage of graft luminal surface occupied by cells, a standardized protocol was established: each conduit was divided into four regions as follows: proximal anastomosis (region A1), ascending aorta (region A2), descending aorta (region B1), and distal anastomosis with the native recipient aorta (region B2), and representative cross sections of each region underwent detailed histomorphological analysis to assess the cellular content and repopulation pattern using built-in functions of NIH ImageJ software, averaging results of the different regions for each graft.

Immunohistological graft analysis. Cryoembedding, sectioning, and fixation were performed as described above. Afterward, cryosections were incubated sequentially for

10 min with 0.25% Triton X-100 and for 1 h with 5% bovine serum albumin +0.1% Tween 20 at room temperature following incubation with primary antibodies (anti-von Willebrand factor [vWF]; DAKO, Glostrup, Denmark; and anti-alpha-smooth muscle actin [α-SMA], Sigma-Aldrich) +1% bovine serum albumin +0.1% Tween 20 for 1 h at 37°C. Secondary antibodies were conjugated to the fluorophore Alexa 488 (α-SMA) and Alexa 546 (vWF; Invitrogen) and incubated (+1% bovine serum albumin +0.1% Tween 20) for 45 min in a dark and humid chamber at 37°C. Sections were covered with VECTASHIELD mounting medium containing DAPI (Vector Labs, Burlingame, CA) and visualized with a fluorescent microscope (DM2000; Leica) and the Leica Application Suite V3.7 software. All chemicals required were obtained from Sigma-Aldrich and Merck.

Matrix metalloproteinase activity via *in situ* zymography. To determine the matrix metalloproteinase (MMP) activity in the explanted functionalized AoGs, *in situ* zymography was performed as previously described.[21] Briefly, cryosections were incubated with 10 μg/mL fluorescein-labeled gelatin (Invitrogen) in 50 mM Tris–HCl, 10 mM $CaCl_2$, 150 mM NaCl, and 5% Triton X-100 for 20 h at room temperature. Sections were mounted with VECTASHIELD medium containing DAPI, and MMP gelatinase activity was visualized by fluorescence microscopy imaging as described above. Specificity of gelatinase activity was confirmed by incubation with gelatin in the presence of 20 mM EDTA. Comparative quantification of the MMP activity was performed using built-in functions of NIH ImageJ software. All chemicals required were obtained from Sigma-Aldrich and Merck.

Statistics

Data are presented as mean ± standard deviation of the mean for all continuous variables. For direct group comparisons at one single time point, Student's *t*-tests with or without Welch's correction or Mann–Whitney *U* tests were performed. Statistical significance was assumed if *p*-values were lower than 0.05. Data analysis was conducted with GraphPad Prism v5.04 (GraphPad Software, San Diego, CA).

Results

Surface functionalization of dECM

Custom-made bioactive peptides containing three different cell adhesive sequences (RGD, REDV, and YIGSR motifs) were successfully synthesized, purified, and used for surface functionalization of dECM tissue samples (Fig. 1). As proof of concept, surface wettability was assessed by means of CA measurements before and after incubation with RGD for different dECM substrates, such as decellularized ovine pulmonary valvular cusps (dPVCs), decellularized ovine pericardium (dOP), and commercially available ECM (cBP), serving as control (Fig. 2A). Apparent static CAs of dPVCs and dOP significantly decreased after peptide incubation (75.6°± 6.0 vs. 51.1°± 8.0 and 77.5°± 2.5 vs. 50.5°± 5.9, respectively, $p < 0.05$), while CAs of cBP did not change (46.0°± 5.8 vs. 52.9°± 4.6, $p > 0.05$) (Fig. 2B). The increase in wettability, displayed by the decreasing CA values of dPVCs and dOP after peptide incubation, indicates successful functionalization of freshly decellularized ECM, while the peptides seemed not efficient at functionalizing chemically preserved ECM (cBP) under the same conditions.

To directly verify the presence of the bioactive peptides on the dECM surface, the custom-made peptides were modified at their N-termini with carboxyfluorescein, thereby allowing their visualization by fluorescence microscopy. All fluorescent-labeled peptides (CF-RGD, CF-REDV, and CF-YIGSR) could be detected on dPVCs showing a ubiquitous and uniform distribution on the dECM surface (Fig. 3A). Semiquantitative analysis of absolute fluorescence intensity revealed a concentration-dependent attachment pattern, reaching saturation of labeling signal at around 200 μM for all three peptides, with a slightly higher attachment rate of the CF-YIGSR compared to the CF-RGD and CF-REDV (Fig. 3B).

EC adhesion in vitro

Biological effect of functionalization with cell adhesive motifs was evaluated by analyzing early EC adhesion onto functionalized dECM in a standardized *in vitro* model. Therefore, dPVCs were functionalized with either single RDG, REDV, and YIGSR or a combination of RGD–YIGSR or RGD–REDV at 100 μM concentration and surface seeded with HUVECs (3×10^5 cells/mL) assessing the total area occupied by cells (TAOC) after 1 and 4 h (Fig. 4A).

Functionalization with single peptides did not show a significant difference as assessed by the TAOC compared to a nonfunctionalized control group after 1 and 4 h (TAOC at 1 h: RGD: 17.5% ± 0.3%, REDV: 19.3% ± 11.5%, YIGSR: 16.1% ± 7.4%, and control: 18.5% ± 5.2%, and at 4 h: RGD: 29.2% ± 0.4%, REDV: 26.2% ± 6.0%, YIGSR: 28.4% ± 5.6%, and control: 24.3% ± 6.6%) (Fig. 4B, C). Nonetheless, a trend toward increased early EC adhesion could be observed after 4 h of incubation in the samples functionalized with the peptides. This trend was clearly enhanced when dPVCs were functionalized with peptide combinations (TAOC at 1 h: RGD–YIGSR: 34.1% ± 10.1% and RGD–REDV: 31.8% ± 10.8%), reaching statistical significance at 4 h for the RGD–REDV combination (TAOC at 4 h: RGD–YIGSR: 32.5% ± 7.8% and RGD–REDV: 42.5% ± 3.7%*; *$p < 0.05$ to control).

Endothelialization in vivo

For *in vivo* validation of enhanced dECM endothelialization via biofunctionalization as observed in the previous *in vitro* experiments, a chronic small animal model of infrarenal AoG transplantation with physiological blood flow and pressure challenge was used.[7] dAoGs were functionalized with a combination of RGD–REDV at 100 μM concentration—in analogy to the *in vitro* experiments, heterotopically implanted to the systemic circulation (Fig. 5A) of recipient rats and explanted at 2, 7, 10, and 14 days to evaluate the biological effect on early endothelialization.

Operative outcome and implant function. A total of 49 rats were operated, with 27 rats receiving a functionalized dAoG and 22 rats a nonfunctionalized dAoG, serving as a control group. Overall mortality was 6% ($n = 1$ for functionalized dAoG group and $n = 2$ for control group). Mean operative time was 102.02 ± 6.30 min, and mean abdominal aortic cross-clamp time was 51.10 ± 4.44 min. There were no procedure-related differences in between groups. All recipient rats reaching the explantation time point showed normal

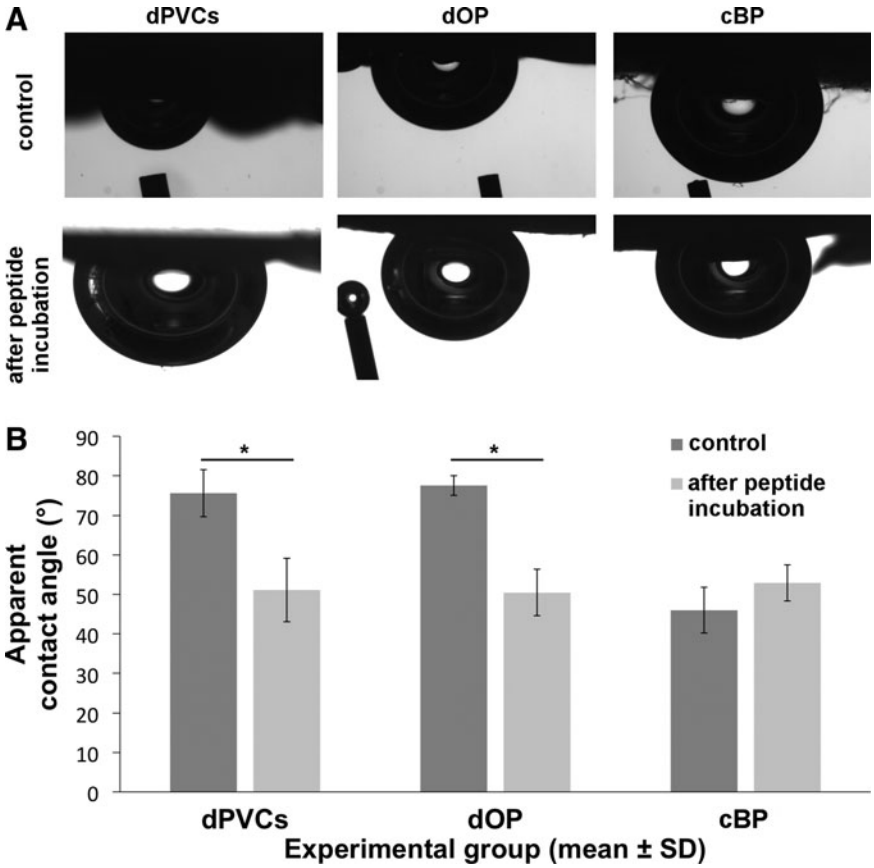

FIG. 2. Wettability of dECM before and after RGD peptide functionalization. **(A)** Representative images of the air bubble/liquid/solid system, where the air bubble was deposited onto the dECM surface with the captive bubble technique. **(B)** Comparison of apparent CAs on respective dECM surfaces before and after functionalization with RGD peptide showing an increase in wettability for freshly dECM and a stationary wettability for chemically preserved commercially available dECM after functionalization (apparent CA [°], mean ± SD; $*p < 0.05$). CA, contact angle; cBP, control bovine pericardium; dECM, decellularized extracellular matrix; dOP, decellularized ovine pericardium; dPVCs, decellularized ovine pulmonary heart valve cusps; SD, standard deviation.

clinical function with adequate somatic growth and gain in body weight and no clinical or Doppler sonographic signs of lower body malperfusion. PSV of blood flow measured at the proximal and distal graft sites decreased over time (proximal: 208.13 ± 22.42 cm/s and distal: 172.07 ± 18.58 cm/s at explantation), with Doppler sonographic graft patency demonstrated at all measured time points (Fig. 5A). At explantation, graft patency was 100% for all functionalized as well as nonfunctionalized explanted dAoGs.

Persistence of biofunctionalization *in vivo*. To assess whether functionalization of dAoGs persisted under systemic circulation and exposure to native plasmatic enzymes in our *in vivo* model system, dAoGs functionalized with fluorescent-labeled peptides (CF-RDG/CF-REDV) were implanted as described above and explanted at 2 and 10 days ($n = 3$, respectively). Fluorescence imaging before implantation revealed completely fluorescent dAoGs, with homogeneous and complete fluorescence throughout all graft layers.

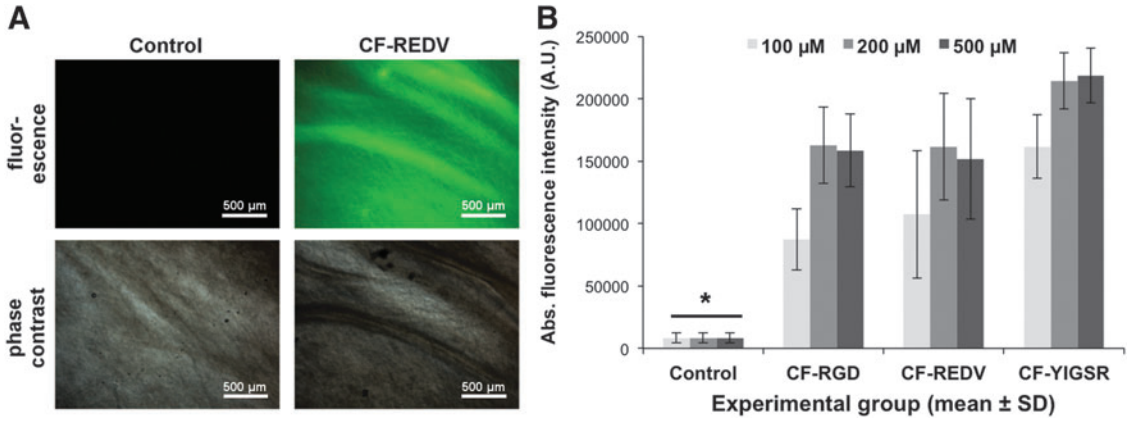

FIG. 3. Biofunctionalization of dPVCs with carboxyfluorescein-labeled peptides. **(A)** Representative images of dPVCs functionalized with nonlabeled REDV (control) and carboxyfluorescein-labeled CF-REDV under fluorescence imaging and phase contrast, respectively. Carboxyfluorescein labeling, *green*. **(B)** Semiquantitative analysis of absolute fluorescence intensity of dPVCs functionalized with carboxyfluorescein-labeled CF-RGD, CF-REDV, and CF-YIGSR and nonfunctionalized controls at 100, 200, and 500 µM peptide concentrations (absolute fluorescence intensity, mean ± SD; $*p < 0.0001$). Color images available online at www.liebertpub.com/tec

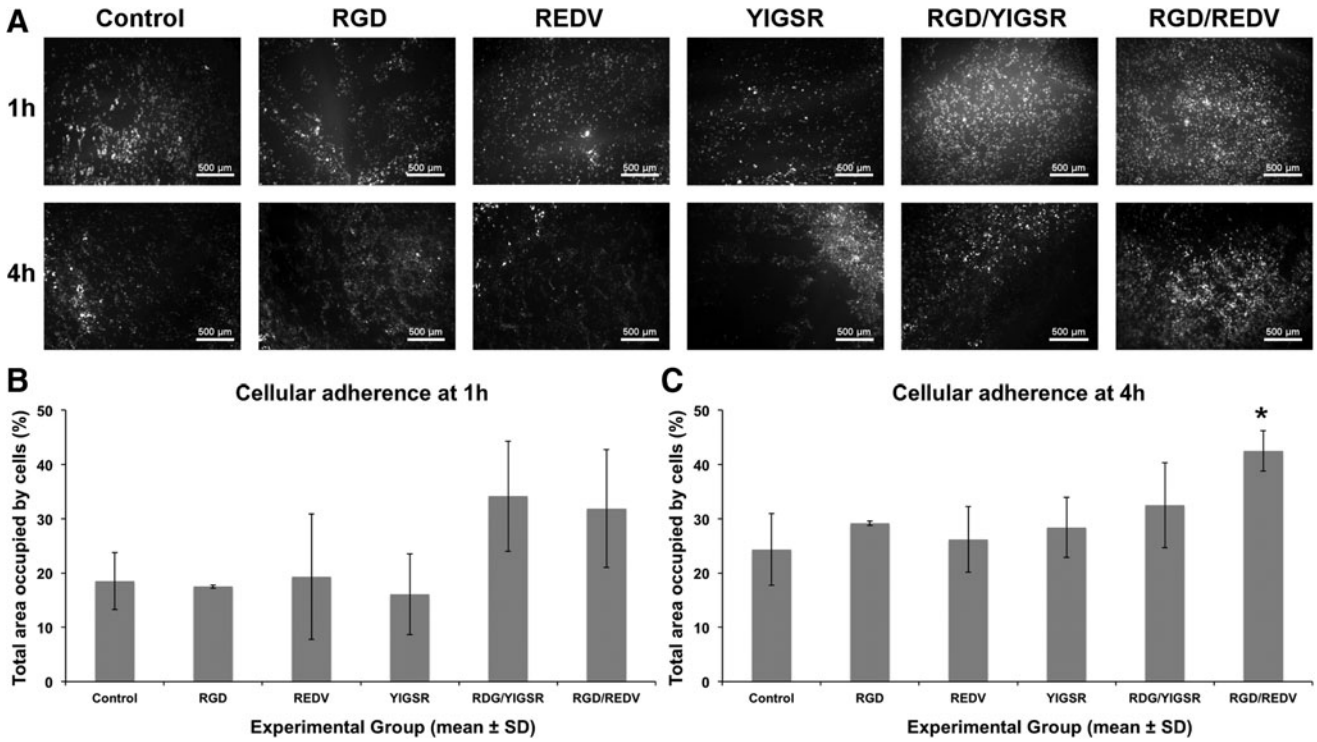

FIG. 4. Cellular adherence onto functionalized dPVCs. **(A)** Representative contrast-enhanced *gray* scale images of HUVEC adherence (3×10^5 cells/mL) onto functionalized dPVCs at 1 and 4 h. As explained in the ''*In Vitro* Cell Adhesion Studies'' section for semiquantitative analysis, each image was further divided into 36 ROI with individual threshold settings accounting for in-sample inhomogeneity and variance due to nonflat surface and fluorescence dispersion. **(B, C)** Semiquantitative analysis of total area occupied by cells at 1 and 4 h, respectively (%, mean ± SD; $*p < 0.05$). HUVEC, human umbilical vein endothelial cell; ROI, region of interest.

Homogeneous fluorescent signal on fluorescent-labeled and functionalized grafts was persistent after 2 and 10 days *in vivo*, however, with a slight decrease in fluorescent intensity (Fig. 5B).

Endothelium formation. Although histological evaluation of explanted dAoGs (Fig. 6) showed cellular graft infiltration starting at the adventitia and sporadically reaching the media after 48 h, semiquantitative analysis revealed no significant formation of endothelium on dAoGs after 2 and 7 days *in vivo* ($n = 3$, respectively), neither in the functionalized nor in the nonfunctionalized control group, with only sporadic cells on the graft luminal surface (Fig. 7A). Initial signs of relevant endothelium formation became apparent after 10 days *in vivo* with 4.6% ± 5.7% of the luminal diameter covered with cells in the RGD/REDV-functionalized dAoGs as opposed to 2.6% ± 3.7% in the nonfunctionalized control group ($n = 7$, respectively) (Fig. 7A).

After 14 days, *in vivo* endothelium formation of RGD/REDV-functionalized dAoGs already reached one fourth of the assessed luminal graft surface, while only one fifth of the luminal graft surface of the nonfunctionalized control group was covered with cells (luminal diameter covered with endothelium: 25.8% ± 9.3% in the RGD/REDV-functionalized group vs. 19.1% ± 14.1% in the nonfunctionalized group; $n = 7$, respectively). However, despite a trend toward enhanced endothelialization in the functionalized group, this effect failed to reach statistical significance within the limited *n* size of the groups and the observed biological variability (Fig. 7A). Regional graft analysis revealed endothelium formation to be particularly enhanced by RGD/REDV functionalization in the proximal and distal (anastomosis near) graft sites, however, without reaching statistical significance compared to the control group (luminal diameter covered with endothelium; region A1: 42.7% ± 27.1% vs. 27.9% ± 27.5%; region B1: 14.9% ± 25.7% vs. 9.5% ± 11.1%; RGD/REDV-functionalized group vs. nonfunctionalized group, respectively) (Fig. 7B). Additionally, there was a trend toward increased overall graft recellularization in the RGD/REDV-functionalized group compared to the nonfunctionalized control group (absolute area occupied by cell nuclei [arbitrary units], 170.6 ± 67.7 in the RGD/REDV-functionalized group vs. 151.1 ± 110.2 in the nonfunctionalized group; $n = 7$, respectively) (Supplementary Fig. S2).

After 14 days, *in vivo* signs of early intimal hyperplasia were already apparent in the explanted grafts. A thorough analysis of all explants was performed to assess the nature and a possible intergroup difference regarding the neointimal characteristics. The ratio of multilayered hyperplastic endothelium to single-layer endothelium was increased in the functionalized group, with 19.7% ± 22.2% versus 9.2% ± 9.0% of the evaluated luminal graft diameter covered with hyperplastic endothelium in the respective RGD/REDV-functionalized and nonfunctionalized control groups (Fig. 7C).

Immunofluorescent staining revealed vWF-positive cells in the newly formed endothelium in both groups, while

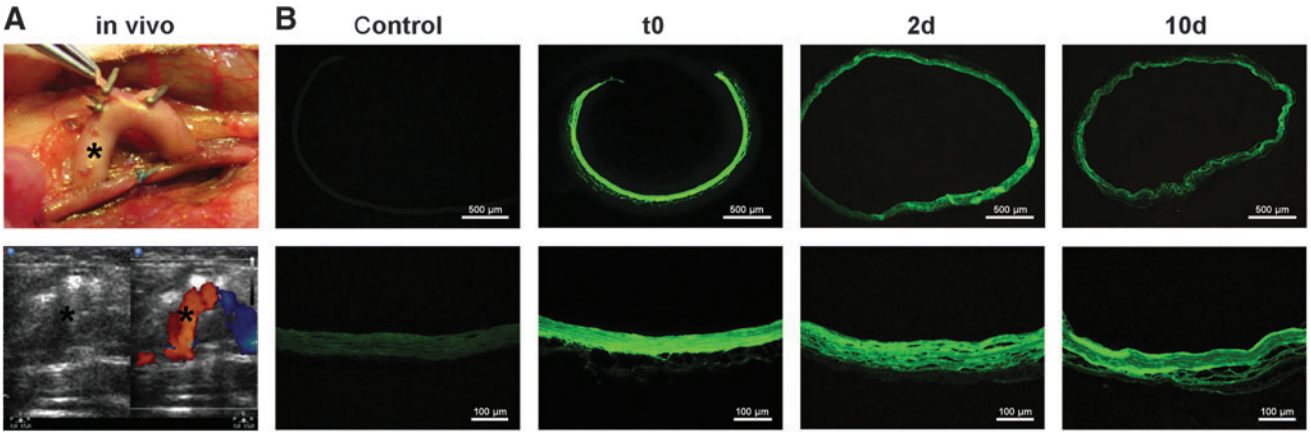

FIG. 5. *In vivo* persistence of biofunctionalization in a functional rodent aortic transplantation model. **(A)** Representative macroscopic and Doppler sonographic image of an infrarenal implanted dAoG showing a functional graft. *dAoG. **(B)** Representative fluorescent images of a nonlabeled RGD/REDV-functionalized graft (control) showing slight autofluorescence, as well as carboxyfluorescein-labeled CF-RGD/CF-REDV-functionalized grafts before implantation (t0) and after 2 and 10 days *in vivo* showing homogeneous and complete fluorescence throughout all graft layers with a slight decrease in fluorescence intensity over time, demonstrating *in vivo* persistence of biofunctionalization. dAoG, decellularized aortic graft. Color images available online at www.liebertpub.com/tec

medium-repopulating cells stained positive for α-SMA (Fig. 8A, B). However, α-SMA-positive cells could also be found in areas of multilayered hyperplastic endothelium, as well as in seemingly single-layer endothelium. Additionally, *in situ* zymography demonstrated high MMP activity, as expected, not only around medium-repopulating cells and hyperplastic endothelium but also within the single-layered ECs (Fig. 8C, D and Supplementary Fig. S3). MMP activity analyzed via semiquantitative analysis showed high in-sample and in-group variability, with, however, consistent high activity at an endothelial level but with no statistical difference between groups (data not shown).

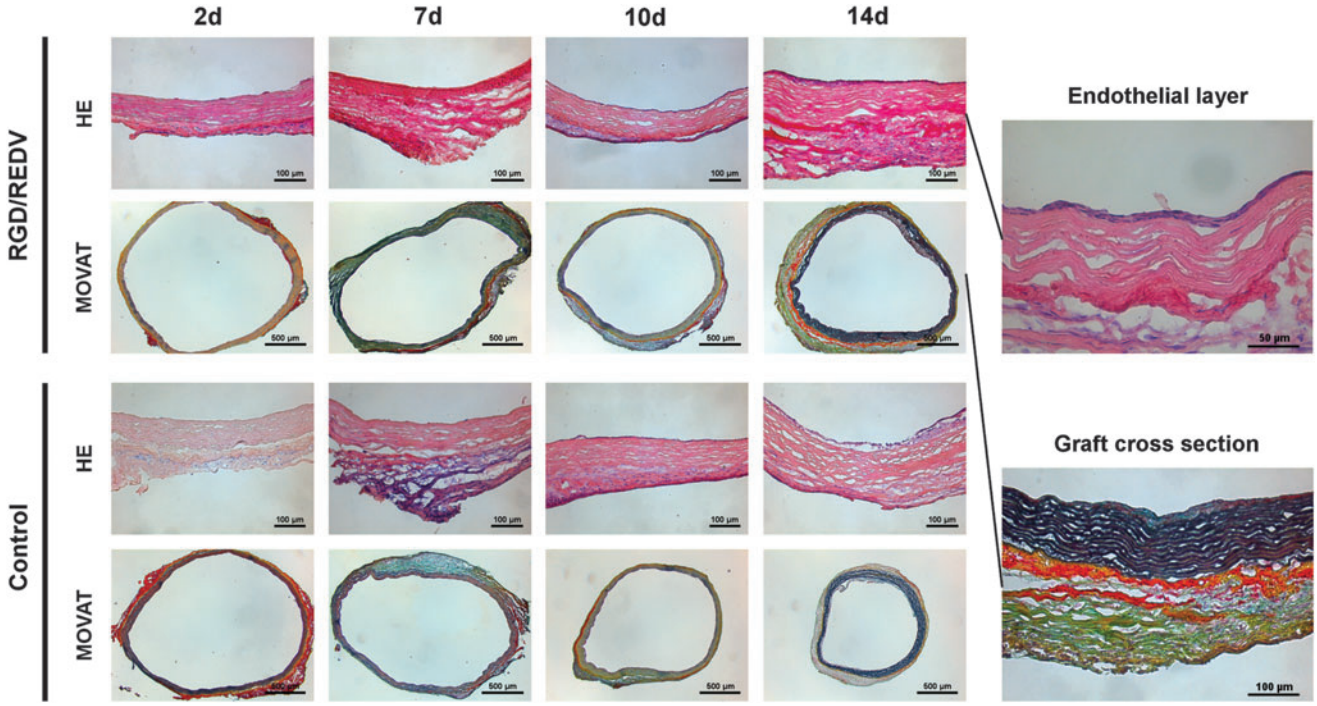

FIG. 6. *In vivo* endothelialization I. Representative images of HE and Movat's pentachrome-stained explanted RGD/REDV-functionalized and nonfunctionalized dAoGs after 2, 7, 10, and 14 days *in vivo*, respectively, showing the beginning of endothelium formation starting at day 10. Additional representative higher magnitude cross section of RGD/REDV-functionalized graft after 14 days *in vivo* showing endothelial layer on the luminal graft side (HE stain) and varying ECM compositions depending on graft region (Movat's stain). ECM, extracellular matrix; HE, hematoxylin and eosin. Color images available online at www.liebertpub.com/tec

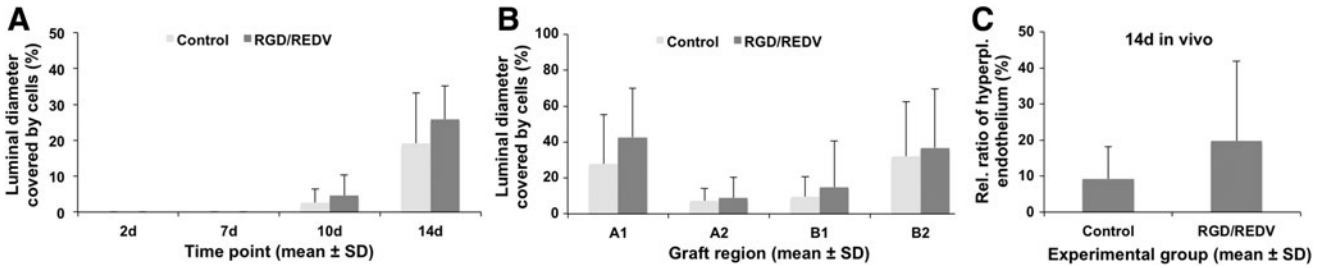

FIG. 7. *In vivo* endothelialization II. Functionalization of dAoGs implanted in functional aortic transplantation model shows a trend toward enhanced *in vivo* endothelialization and hyperplastic endothelium formation. **(A)** Semiquantitative analysis of luminal graft diameter covered by cells of explanted RGD/REDV-functionalized and nonfunctionalized (control) dAoGs after 2, 7, 10, and 14 days *in vivo* (%, mean ± SD). **(B)** Semiquantitative analysis of regional luminal graft diameter covered by cells of explanted RGD/REDV-functionalized and nonfunctionalized dAoGs after 14 days *in vivo*. A1, proximal anastomosis; B2, distal anastomosis (%, mean ± SD). **(C)** Relative ratio of multilayered hyperplastic endothelium to single-layer endothelium in explanted RGD/REDV-functionalized and nonfunctionalized dAoGs after 14 days *in vivo* (%, mean ± SD).

Discussion

Customized biofunctionalization of decellularized ECM

Targeted functionalization of interfaces to increase biocompatibility is a widely explored approach in material science.[15–18] As shown in previous reports, using defined short bioactive sequences rather than large proteins as biological active agents, it is possible to achieve surface functionalization with defined control of biological interaction and high cell specificity.[15,23,24] However, customized interface biofunctionalization with synthetic peptides has essentially been applied to synthetic nonbiological materials as they usually have biologically inert interfaces with homogeneous surfaces allowing controlled peptide anchoring.[25,32,41,42] In the case of native-derived ECM materials, interface modification is usually neglected or gross surface coating with large unselective proteins is performed as the interface is already constituted by biologically active ECM proteins with an inhomogeneous and anisotropic surface complicating complex functionalization strategies.[43] Therefore, in this proof-of-concept study, we specifically designed and synthesized custom-made peptides with interchangeable bioactive motifs containing a spacing-anchoring moiety to ensure appropriate binding as well as orientation of the bioactive motifs on dECM substrates. To the best of the authors' knowledge, this is the first study showing customized biofunctionalization of dECM with tailor-made synthetic peptides allowing full control of biological potential by targeted bioactive sequence selection.

Validation of custom-made peptide binding onto decellularized ECM

Peptide binding on dECM surfaces was confirmed and analyzed by CA measurements and fluorescent microscopy. Other techniques commonly used to characterize biomolecule binding to synthetic surfaces, such as X-ray photoelectron spectroscopy (XPS), quartz crystal microbalance with dissipation monitoring (QCM-D), or optical waveguide lightmode spectroscopy (OWLS), could not be used owing to the intricate nature of dECM substrates.

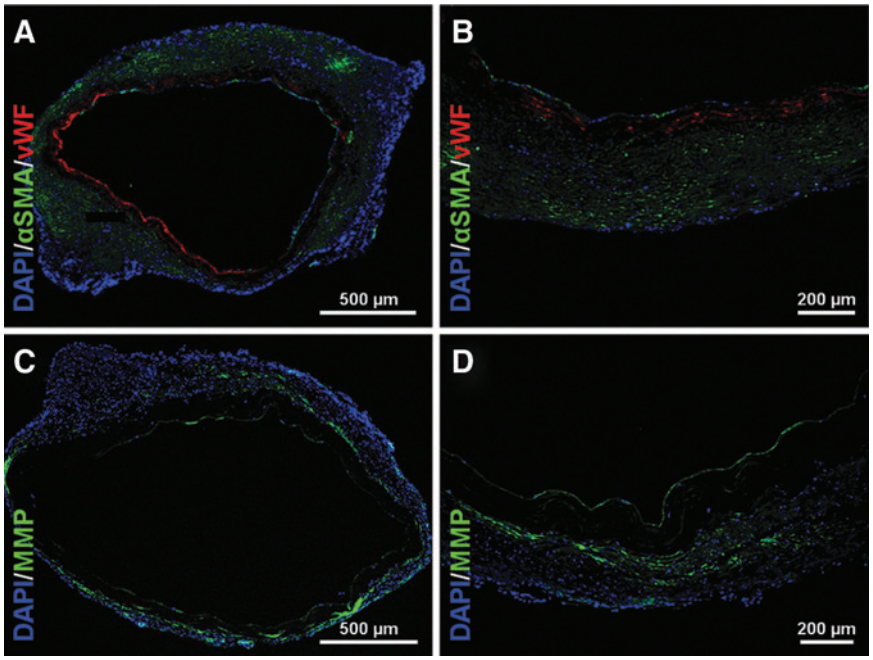

FIG. 8. *In vivo* endothelialization III. **(A, B)** Representative immunofluorescent images of explanted RGD/REDV-functionalized dAoGs after 14 days *in vivo* showing vWF-positive cells on the inner luminal graft surface and α-SMA-positive cells in the media region. *Blue*, DAPI; *red*, vWF; *green*, α-SMA. **(C, D)** Representative images of *in situ* zymography of explanted RGD/REDV-functionalized dAoGs after 14 days *in vivo* showing MMP activity not only around medium-repopulating cells and hyperplastic endothelium but also within the single-layered ECs. *Blue*, DAPI; *green*, MMP-active regions. α-SMA, alpha-smooth muscle actin; ECs, endothelial cells; MMP, matrix metalloproteinase; vWF, von Willebrand factor. Color images available online at www.liebertpub.com/tec

CA measurements allow the detection of minor changes in the surface composition or morphology[40,44] and thus are frequently used to monitor protein adsorption and the functionalization of diverse substrates. To fully preserve the integrity of dECM samples, dPVCs were immersed in distilled water, and CA was measured using the captive bubble technique. This approach proved useful to analyze the wettability of this type of substrate. In particular, wettability of dPVCs and dOPs significantly increased after RGD functionalization despite the heterogeneity and roughness of dECM samples, suggesting the efficiency of the biofunctionalization process. This finding is consistent with the presence of polar guanidine and carboxyl groups present in the sequence of the bioactive RGD biomolecule. In contrary, apparent CA measurements in cBP, already indicating a different wettability compared to dECM, did not change before and after peptide functionalization, indicating a lower efficiency of the functionalization process as expected due to the chemical preservation of the commercially available ECM by incubation in an alcohol solution.

Fluorescent labeling of the peptides via incorporation of 5(6)-carboxyfluorescein into the peptide sequence and fluorescent analysis of the functionalized dECM substrates directly confirmed CA measurements and allow quantifying the extent of peptide binding. Interestingly, fluorescence imaging revealed the fluorescent-labeled peptides to be present throughout all dAoG vascular graft layers, exceeding simple surface coating. This may be explained by the small molecular size and the porosity of the dECM,[45] leading to peptide diffusion throughout the ECM scaffold. Additionally, the hydrophobic aminohexanoic acid residues present in the synthetic peptides might also contribute to improve the retention of the peptide via hydrophobic interactions with the substrates. As previously reported, dECM scaffolds are rich in collagenous proteins,[1,2,8] which contain a high abundance of hydrophobic amino acids (i.e., alanine, glycine, and proline), and could therefore favor these interactions. According to the scale of hydrophilicity described by Hopp and Woods,[46] values of hydrophilicity for RGD, REDV, and YIGSR peptides are 6.3, 7.5, and −0.8, respectively, indicating a strong hydrophobic character for YIGSR. This is concordant to our observation that this peptide most efficiently immobilized on the dPVCs compared to the other sequences.

Furthermore, custom-made peptides could be detected within dAoG vascular grafts up to 10 days under systemic circulation and despite exposure to native plasmatic enzymes in our *in vivo* model system, ensuring peptide presence at the beginning of the *in vivo* endothelialization process. This observation is highly relevant because it demonstrates that our functionalization strategy does provide a stable binding of the peptides to the dECM substrate even under *in vivo* conditions.

Evaluation of biological effects of functionalization of decellularized ECM via custom-made synthetic peptides

The observed binding of custom-made synthetic peptides onto dECM translated into a measurable biological response *in vitro*, demonstrating the feasibility of customized dECM biofunctionalization. Particularly, dual functionalization by combining peptides containing the Arg-Gly-Asp (RGD) sequence with those containing either the Arg-Glu-Asp-Val (REDV) sequence or the Tyr-Ile-Gly-Ser-Arg (YIGSR) sequence increased EC adhesion *in vitro* compared to mono- or nonfunctionalized controls. The best combination was the equimolar mixture of RGD with REDV, which yielded statistically higher values of EC adhesion after 4 h of incubation in comparison to control. The capacity of the REDV sequence to mediate EC adhesion through integrin $\alpha_4\beta_1$ supports the observed synergistic biological effect.[46,47] Those findings were concordant to previous reports, demonstrating that specificity of functionalization can be augmented by targeted bioactive sequence selection and combinatory application thereof.[15,22,25,39,48]

Validation in a functional rodent aortic transplantation model under physiological flow conditions and full exposure to the native blood[7] failed to show a significant biological effect despite showing *in vivo* persistence of the dECM functionalization. Although a trend toward increased *in vivo* endothelialization of the functionalized dAoGs compared to the nonfunctionalized controls could be observed, it failed to reach statistical significance within the number of animals subjected to our model system and due to observed large biological variability of the early endothelialization process, which was also evident in the control group.

Additional findings of this study although still circumstantiate the biological effects of RDG/REDV functionalization, there was a trend of increased overall graft recellularization—coherent with the peptide presence throughout all graft layers—and enhancement of neointimal hyperplasia in the functionalized dAoGs. This is consistent with previous *in vivo* findings, in which adventitial bioactive coating of dAoGs stimulated repopulation of the media region[21] and luminal fibronectin or RGD coating triggered neointima formation.[21,49] Nonetheless, further studies are warranted, evaluating the possible effects of customized biofunctionalization of dECM on *in vivo* endothelialization.

Biological potential of custom-made synthetic peptides for the functionalization of decellularized ECM

Biological potential of ECM-derived protein coating of dECM has already been demonstrated in the past, with, for example, fibronectin coating accelerating autologous graft recellularization.[21] However, protein-based coatings may prove insufficient to selectively elicit specific biological cues potentially required in the process of neoendothelium formation, thus failing in providing functional endothelium.[21] This is concordant with the intrinsic limitations associated with the use of full-length proteins as coating molecules, which include low specificity, limited stability, and immunogenicity.[24] Thus, newer strategies aiming at circumventing the limitations of classical protein-based methods are warranted in the design of functional biological grafts.

This study demonstrates that a high degree of customization in dECM functionalization can be achieved by the presented approach, whereas the combination of targeted peptide motifs may simplify the complexity of natural ECM proteins while improving the biological activity of single peptides, for example, increasing the specificity of substrate functionalization. Advanced multiactive peptide platforms based on the design presented in this study and with the capacity to simultaneously present two distinct bioactive peptide motifs in a chemically defined manner have already

been successfully synthesized and used on non-ECM materials.[25] As demonstrated in this study, dECM functionalization via synthetic peptides is feasible, so that using those advanced platforms further controls selective bioactive sequence presentation, as well as combinations from a wide range of biologically relevant peptide motifs will become available. Therefore, simultaneous and directed activation of relevant synergistic domains, control of selective cell adhesion, specific regulation of cell differentiation and proliferation, and activation of antifouling and/or antibacterial properties on dECM may become possible.

Implications for cardiovascular bioengineering

For cardiovascular applications, interface characteristics are highly important as cardiovascular implants usually lie in direct contact to the bloodstream with adverse biological effects, such as thrombosis, intimal hyperplasia, and calcification leading to possible fatal consequences.[50] Therefore, early functional endothelialization is crucial for all non-autologous surfaces in direct contact with the bloodstream. Here, interface functionalization approaches—enhancing *in vivo* autologous recellularization—may omit tedious cell- and bioreactor-based *ex vivo* preimplant procedures[8,51–53] as they may not only enhance EC adhesion to ligands of the basal membrane but also stabilize the neoendothelium in front of shear forces generated by the bloodstream.[53]

Nonetheless, current approaches, although enhancing *in vivo* endothelialization, have failed to prevent and even may lead to increased neointima formation.[21,49] This is particularly important as, for example, in the case of engineered vascular grafts, adverse neovessel remodeling directly leads to early and late graft failure.[13] Here, the integration of antiproliferative motifs preventing smooth muscle cell overproliferation [42] into a customized functionalization approach may pave the way to a new generation of multifunctional dECM scaffolds.

Hence, customized biofunctionalization of dECM with high cell specificity and selectivity in the provoked biological response may have great implications for cardiovascular bioengineering. As a whole concert of biological effects takes place during *in vivo* graft remodeling, directed multilevel control of dECM–blood interfaces may greatly improve cardiovascular implants. Our findings suggest that through the presented dECM biofunctionalization strategy—with an adequate selection and combination of bioactive motifs and advanced peptide platforms—targeted EC specificity of dECM without activation of platelet attachment, immune cell recruitment, and smooth muscle cell overproliferation could possibly be achieved. Furthermore, as shown in this study, custom-made synthetic peptides may also be used to functionalize nonluminal parts of dECM as—due to their small molecular size—they seem to diffuse into the porous ECM. This may open up possibilities to influence graft remodeling through directed cell migration and activation throughout dECM-based grafts, having a great impact especially for the engineering of vascular grafts and heart valves.

Limitations

This study was intended as a proof-of-concept study on the feasibility of customized dECM functionalization via tailor-made synthetic peptides. Although customized functionalization of dECM with selected bioactive peptides adhering to dECM surfaces *in vitro* and up to 10 days in a physiologically functional *in vivo* model could be shown for the first time, biological response in the used *in vivo* model was not as clear as expected, failing to reach statistical significance within the used setting. The reasons may lie not only in the high biological variance of the short observation period compared to similar studies, where the same model was used for considerably longer periods,[21] but also in the selection of bioactive sequences, which may not be the ideal ones when looking at early re-endothelialization in this particular small animal model. Therefore, further studies identifying target bioactive motifs, which will help selectively recruit ECs and prevent neointima formation, are warranted as they could easily be integrated in the presented approach and may lead the way toward enhanced endothelialization.

Conclusions

In this proof-of-concept study, dECM was successfully functionalized with custom-made synthetic peptides showing increased EC attachment on functionalized dPVCs *in vitro* and functionalization persistence under systemic pressure conditions as well as a trend toward enhanced endothelialization of functionalized dAoGs *in vivo*, which, however, failed to reach statistical significance in the used model system. To the best of the authors' knowledge, this is the first study showing customized biofunctionalization of dECM with targeted bioactive sequences. Furthermore, the findings of this study suggest that the biological potential of dECM interface functionalization can be increased by targeted selection and combination of bioactive motifs. Since bioactive sequences within the dECM–synthetic peptide platform are easily interchangeable and combinable, further control of host cell proliferation, function, and differentiation—beyond simple cell attachment—seems feasible. Thus, the presented strategy could pave the way to a new generation of multifunctional dECM scaffolds for regenerative medicine, with particular implications regarding the functional recellularization of engineered vascular grafts and heart valves, possibly leading the way toward enhanced endothelialization strategies.

Acknowledgments

The authors gratefully acknowledge Prof. Dr. Gesine Kögler from the Institute for Transplantation Diagnostics and Cell Therapeutics of the Heinrich-Heine-University for providing the HUVECs and the *Susanne Bunnenberg-Stiftung* (NRW, Germany) for her generous donation to the Research Group for Experimental Surgery of the Department of Cardiovascular Surgery of the Heinrich-Heine-University, which provided a great part of the laboratory infrastructure that was used in this project. Furthermore, the authors acknowledge the Spanish government for financial support through project MAT 2012-30706, cofunded by the EU through European Regional Development Funds, and the Agency for Administration of University and Research Grants of the Government of Catalonia (2014 SGR 1333). C.M.-M. thanks the support of the Secretary for Universities and Research of the Ministry of Economy and Knowledge of the Government of Catalonia (2011-BP-B-00042) and the People Programme (Marie Curie Actions) of the European Union's Seventh Framework Programme (FP7-PEOPLE-2012-CIG, REA Grant Agreement 321985).

Disclosure Statement

No competing financial interests exist.

References

1. Akhyari, P., Aubin, H., Gwanmesia, P., Barth, M., Hoffmann, S., Huelsmann, J., Preuss, K., and Lichtenberg, A. The quest for an optimized protocol for whole-heart decellularization: a comparison of three popular and a novel decellularization technique and their diverse effects on crucial extracellular matrix qualities. Tissue Eng Part C Methods **17,** 915, 2011.
2. Hülsmann, J., Grün, K., El Amouri, S., Barth, M., Hornung, K., Holzfuß, C., Lichtenberg, A., and Akhyari, P. Transplantation material bovine pericardium: biomechanical and immunogenic characteristics after decellularization vs. glutaraldehyde-fixing. Xenotransplantation **19,** 286, 2012.
3. Badylak, S.F. Decellularized allogeneic and xenogeneic tissue as a bioscaffold for regenerative medicine: factors that influence the host response. Ann Biomed Eng **42,** 1517, 2014.
4. Moroni, F., and Mirabella, T. Decellularized matrices for cardiovascular tissue engineering. Am J Stem Cells **3,** 1, 2014.
5. Cebotari, S., Lichtenberg, A., Tudorache, I., Hilfiker, A., Mertsching, H., Leyh, R., Breymann, T., Kallenbach, K., Maniuc, L., Batrinac, A., Repin, O., Maliga, O., Ciubotaru, A., and Haverich, A. Clinical application of tissue engineered human heart valves using autologous progenitor cells. Circulation **114 (1 Suppl),** I132, 2006.
6. Akhyari, P., Kamiya, H., Gwanmesia, P., Aubin, H., Tschierschke, R., Hoffmann, S., Karck, M., and Lichtenberg, A. In vivo functional performance and structural maturation of decellularised allogenic aortic valves in the subcoronary position. Eur J Cardiothorac Surg **38,** 539, 2010.
7. Assmann, A., Akhyari, P., Delfs, C., Flögel, U., Jacoby, C., Kamiya, H., and Lichtenberg, A. Development of a growing rat model for the in vivo assessment of engineered aortic conduits. J Surg Res **176,** 367, 2012.
8. Lichtenberg, A., Tudorache, I., Cebotari, S., Suprunov, M., Tudorache, G., Goerler, H., Park, J.K., Hilfiker-Kleiner, D., Ringes-Lichtenberg, S., Karck, M., Brandes, G., Hilfiker, A., and Haverich, A. Preclinical testing of tissue-engineered heart valves re-endothelialized under simulated physiological conditions. Circulation **114(1 Suppl),** I-559, 2006.
9. da Costa, F.D., Costa, A.C.B., Prestes, R., Domanski, A.C., Balbi, E.M., Ferreira, A.D., and Lopes, S.V. The early and midterm function of decellularized aortic valve allografts. Ann Thorac Surg **90,** 1854, 2010.
10. Simon, P., Kasimir, M.T., Seebacher, G., Weigel, G., Ullrich, R., Salzer-Muhar, U., Rieder, E., and Wolner, E. Early failure of the tissue engineered porcine heart valve SYNERGRAFT® in pediatric patients. Eur J Cardiothorac Surg **23,** 1002, 2003.
11. Keane, T.J., Londono, R., Turner, N.J., and Badylak, S.F. Consequences of ineffective decellularization of biologic scaffolds on the host response. Biomaterials **33,** 1771, 2012.
12. Kasimir, M., Rieder, E., Seebacher, G., Nigisch, A., Dekan, B., Wolner, E., Weigel, G., and Simon, P. Decellularization does not eliminate thrombogenicity and inflammatory stimulation in tissue-engineered porcine heart valves. J Heart Valve Dis **15,** 278, 2006.
13. Seifu, D.G., Purnama, A., Mequanint, K., and Mantovani, D. Small-diameter vascular tissue engineering. Nat Rev Cardiol **10,** 410, 2013.
14. Pankajakshan, D., and Agrawal, D.K. Scaffolds in tissue engineering of blood vessels. Can J Physiol Pharmacol **88,** 855, 2010.
15. de Mel, A., Jell, G., Stevens, M.M., and Seifalian, A.M. Biofunctionalization of biomaterials for accelerated in situ endothelialization: a review. Biomacromolecules **9,** 2969, 2008.
16. Bierbaum, S., Hintze, V., and Scharnweber, D. Functionalization of biomaterial surfaces using artificial extracellular matrices. Biomatter **2,** 132, 2012.
17. von der Mark, K., and Park, J. Engineering biocompatible implant surfaces: Part II: cellular recognition of biomaterial surfaces: lessons from cell–matrix interactions. Prog Mater Sci **58,** 327, 2013.
18. Tejero, R., Anitua, E., and Orive, G. Toward the biomimetic implant surface: biopolymers on titanium-based implants for bone regeneration. Prog Polym Sci **39,** 1406, 2014.
19. Shimada, T., Nishibe, T., Miura, H., Hazama, K., Kato, H., Kudo, F., Murashita, T., and Okuda, Y. Improved healing of small-caliber, long-fibril expanded polytetrafluoroethylene vascular grafts by covalent bonding of fibronectin. Surg Today **34,** 1025, 2004.
20. Zhou, M., Liu, Z., Wei, Z., Liu, C., Qiao, T., Ran, F., Bai, Y., Jiang, X., and Ding, Y. Development and validation of small-diameter vascular tissue from a decellularized scaffold coated with heparin and vascular endothelial growth factor. Artif Organs **33,** 230, 2009.
21. Assmann, A., Delfs, C., Munakata, H., Schiffer, F., Horstkötter, K., Huynh, K., Barth, M., Stoldt, V.R., Kamiya, H., Boeken, U., Lichtenberg, A., and Akhyari, P. Acceleration of autologous in vivo recellularization of decellularized aortic conduits by fibronectin surface coating. Biomaterials **34,** 6015, 2013.
22. Wei, Y., Ji, Y., Xiao, L.L., Lin, Q.K., Xu, J.P., Ren, K.F., and Ji, J. Surface engineering of cardiovascular stent with endothelial cell selectivity for in vivo re-endothelialisation. Biomaterials **34,** 2588, 2013.
23. Shin, H., Jo, S., and Mikos, A.G. Biomimetic materials for tissue engineering. Biomaterials **24,** 4353, 2003.
24. Williams, D.F. The role of short synthetic adhesion peptides in regenerative medicine; the debate. Biomaterials **32,** 4195, 2011.
25. Mas-Moruno, C., Fraioli, R., Albericio, F., Manero, J.M., and Gil, F.J. Novel peptide-based platform for the dual presentation of biologically active peptide motifs on biomaterials. ACS Appl Mater Interfaces **6,** 6525, 2014.
26. Pierschbacher, M.D., and Ruoslahti, E. Cell attachment activity of fibronectin can be duplicated by small synthetic fragments of the molecule. Nature **309,** 30, 1984.
27. Hersel, U., Dahmen, C., and Kessler, H. RGD modified polymers: biomaterials for stimulated cell adhesion and beyond. Biomaterials **24,** 4385, 2003.
28. Hubbell, J.A., Massia, S.P., Desai, N.P., and Drumheller, P.D. Endothelial cell-selective materials for tissue engineering in the vascular graft via a new receptor. Nat Biotechnol **9,** 568, 1991.
29. Veiseh, M., Veiseh, O., Martin, M.C., Asphahani, F., and Zhang, M. Short peptides enhance single cell adhesion and viability on microarrays. Langmuir **23,** 4472, 2007.
30. Massia, S.P., and Hubbell, J.A. Convalent surface immobilization of Arg-Gly-Asp-and Tyr-Ile-Gly-Ser-Arg-containing peptides to obtain well-defined cell-adhesive substrates. Anal Biochem **187,** 292, 1990.
31. Jun, H.W., and West, J.L. Modification of polyurethaneurea with PEG and YIGSR peptide to enhance endothelialization

without platelet adhesion. J Biomed Mater Res B Appl Biomater **72,** 131, 2005.
32. Mas-Moruno, C., Dorfner, P.M., Manzenrieder, F., Neubauer, S., Reuning, U., Burgkart, R., and Kessler, H. Behavior of primary human osteoblasts on trimmed and sandblasted Ti6Al4V surfaces functionalized with integrin αvβ3-selective cyclic RGD peptides. J Biomed Mater Res A **101,** 87, 2013.
33. Pallarola, D., Bochen, A., Boehm, H., Rechenmacher, F., Sobahi, T.R., Spatz, J.P., and Kessler, H. Interface immobilization chemistry of cRGD-based peptides regulates integrin mediated cell adhesion. Adv Funct Mater **24,** 943, 2014.
34. El-Faham, A., and Albericio, F. Peptide coupling reagents, more than a letter soup. Chem Rev **111,** 6557, 2011.
35. Fernández-Carneado, J., Kogan, M.J., Castel, S., and Giralt, E. Potential peptide carriers: amphipathic proline-rich peptides derived from the N-terminal domain of γ-zein. Angew Chem Int Ed Engl **43,** 1811, 2004.
36. Lauten, A., Laube, A., Schubert, H., Bischoff, S., Nietzsche, S., Horstkötter, K., Poudel-Bochmann, B., Franz, M., Lichtenberg, A., Figulla, H.R., and Akhyari, P. Transcatheter treatment of tricuspid regurgitation by caval valve implantation—experimental evaluation of decellularized tissue valves in central venous position. Catheter Cardiovasc Interv **85,** 150, 2015.
37. Akhyari, P., Ziegler, H., Gwanmesia, P., Barth, M., Schilp, S., Huelsmann, J., Hoffmann, S., Bosch, J., Kögler, G., and Lichtenberg, A. A novel culture device for the evaluation of three-dimensional extracellular matrix materials. J Tissue Eng Regen Med **8,** 673, 2014.
38. Aubin, H., Kranz, A., Hülsmann, J., Lichtenberg, A., and Akhyari, P. Decellularized whole heart for bioartificial heart. In: Kao R.L., ed. Cellular Cardiomyoplasty. New York, NY: Humana Press, 2013, pp. 163–178.
39. Castellanos, M.I., Zenses, A.S., Grau, A., Rodríguez-Cabello, J.C., Gil, F.J., Manero, J.M., and Pegueroles, M. Biofunctionalization of REDV elastin-like recombinamers improves endothelialization on CoCr alloy surfaces for cardiovascular applications. Colloids Surf B Biointerfaces **127,** 22, 2015.
40. Drelich, J., Miller, J.D., and Good, R.J. The effect of drop (bubble) size on advancing and receding contact angles for heterogeneous and rough solid surfaces as observed with sessile-drop and captive-bubble techniques. J Colloid Interface Sci **179,** 37, 1996.
41. Joner, M., Cheng, Q., Schönhofer-Merl, S., Lopez, M., Neubauer, S., Mas-Moruno, C., Laufer, B., Kolodgie, F.D., Kessler, H., and Virmani, R. Polymer-free immobilization of a cyclic RGD peptide on a nitinol stent promotes integrin-dependent endothelial coverage of strut surfaces. J Biomed Mater Res B Appl Biomater **100,** 637, 2012.
42. Rechenmacher, F., Steigerwald, K., Laufer, B., Neubauer, S., Kapp, T.G., Li, L., Mas-Moruno, C., Joner, M., and Kessler, H. The integrin ligand c (RGDf (NMe) Nal) reduces neointimal hyperplasia in a polymer-free drug-eluting stent system. ChemMedChem **9,** 1413, 2014.
43. Londono, R., and Badylak, S.F. Biologic scaffolds for regenerative medicine: mechanisms of in vivo remodeling. Ann Biomed Eng **43,** 577, 2015.
44. Pegueroles, M., Gil, F.J., Planell, J.A., and Aparicio, C. The influence of blasting and sterilization on static and time-related wettability and surface-energy properties of titanium surfaces. Surf Coat Technol **202,** 3470, 2008.
45. Brown, B.N., Barnes, C.A., Kasick, R.T., Michel, R., Gilbert, T.W., Beer-Stolz, D., Castner, D.G., Ratner, B.D., and Badylak, S.F. Surface characterization of extracellular matrix scaffolds. Biomaterials **31,** 428, 2010.
46. Hopp, T.P., and Woods, K.R. Prediction of protein antigenic determinants from amino acid sequences. Proc Natl Acad Sci U S A **78,** 3824, 1981.
47. Massia, S.P., and Hubbell, J.A. Vascular endothelial cell adhesion and spreading promoted by the peptide REDV of the IIICS region of plasma fibronectin is mediated by integrin alpha 4 beta 1. J Biol Chem **267,** 14019, 1992.
48. Monchaux, E., and Vermette, P. Bioactive microarrays immobilized on low-fouling surfaces to study specific endothelial cell adhesion. Biomacromolecules **8,** 3668, 2007.
49. Bastijanic, J.M., Marchant, R.E., Kligman, F., Allemang, M.T., Lakin, R.O., Kendrick, D., Kashyap, V.S., and Kottke-Marchant, K. First in vivo evaluation of biomimetic fluorosurfactant polymer-coated expanded polytetrafluoroethylene vascular grafts in a porcine carotid artery bypass model. J Vasc Surg pii:S0741–5214(15)00217-7, 2015.
50. Jaganathan, S.K., Supriyanto, E., Murugesan, S., Balaji, A., and Asokan, M.K. Biomaterials in cardiovascular research: applications and clinical implications. BioMed Res Int **2014,** 459465, 2014.
51. Griese, D.P., Ehsan, A., Melo, L.G., Kong, D., Zhang, L., Mann, M.J., Pratt, R.E., Mulligan, R.C., and Dzau, V.J. Isolation and transplantation of autologous circulating endothelial cells into denuded vessels and prosthetic grafts implications for cell-based vascular therapy. Circulation **108,** 2710, 2003.
52. Lichtenberg, A., Tudorache, I., Cebotari, S., Ringes-Lichtenberg, S., Sturz, G., Hoeffler, K., Hurscheler, C., Brandes, G., Hilfiker, A., and Haverich, A. In vitro re-endothelialization of detergent decellularized heart valves under simulated physiological dynamic conditions. Biomaterials **27,** 4221, 2006.
53. Lichtenberg, A., Cebotari, S., Tudorache, I., Sturz, G., Winterhalter, M., Hilfiker, A., and Haverich, A. Flow-dependent re-endothelialization of tissue-engineered heart valves. J Heart Valve Dis **15,** 287, 2006.

Address correspondence to:
Marta Pegueroles, PhD
Biomaterials, Biomechanics
and Tissue Engineering Group
Department of Materials Science
and Metallurgical Engineering
Technical University of Catalonia
Av. Diagonal 647
08028 Barcelona
Spain

E-mail: marta.pegueroles@upc.edu

Artur Lichtenberg, MD
Department of Cardiovascular Surgery
Heinrich-Heine-University Düsseldorf
Moorenstr. 5
40225 Düsseldorf
Germany

E-mail: artur.lichtenberg@med.uni-duesseldorf.de

Received: December 16, 2015
Accepted: March 15, 2016
Online Publication Date: April 25, 2016